Vol. 736: 35–46, 2024
https://doi.org/10.3354/meps14587

MARINE ECOLOGY PROGRESS SERIES
Mar Ecol Prog Ser

Published May 23



# Eelgrass meadow response to heat stress. I. Temperature threshold for ecosystem production derived from *in situ* aquatic eddy covariance measurements

**Amelie C. Berger*, Peter Berg**

**Department of Environmental Sciences, University of Virginia, Charlottesville, VA 22903, USA**

ABSTRACT: As seagrass meadows are increasingly threatened by warming oceans and extreme heating events, it is critical that we enhance our understanding of their ecosystem response to heat stress. This study relied on our extensive database of hourly eelgrass *Zostera marina* ecosystem metabolism to determine, for the first time, the temperature stress threshold ($T_{th}$) of *Z. marina* meadows under naturally varying *in situ* conditions. Eelgrass ecosystem metabolism was measured using the aquatic eddy covariance technique in a 20 $km^2$ meadow at the Virginia Coast Reserve (USA). We constructed and fitted a non-linear multivariate model to identify 28.6°C as the threshold above which substantial negative effects on net photosynthesis occur. On average, daytime oxygen fluxes decreased by 50% on afternoons when $T_{th}$ was exceeded, which shifted daily net ecosystem metabolism from metabolic balance to net heterotrophy and therefore a loss in carbon. This study highlights the vulnerability of eelgrass meadows to future warming projections.

KEY WORDS: Heat stress · Thermal tolerance threshold · Eelgrass · *In situ* ecosystem metabolism · Aquatic eddy covariance

## 1. INTRODUCTION

Seagrass meadows provide valuable ecosystem services to coastal areas (e.g. Costanza et al. 1997, Beck et al. 2001, Koch et al. 2009) and play an important role as significant carbon sinks in the global carbon cycle, due to high rates of primary production and carbon burial in their sediments (Duarte et al. 2010, Fourqurean et al. 2012, Oreska et al. 2017). However, seagrass ecosystems worldwide have been declining in part due to increasing global temperatures and local extreme events during which water temperatures exceed the thermal tolerance limits of the species (e.g. Moore & Jarvis 2008, Marbá & Duarte 2010, Arias-Ortiz et al. 2018, Berger et al. 2020). Such die-off events not only cause the loss of seagrass ecosystem services but also trigger substantial $CO_2$ emissions from seagrass meadows through the remineralization of previously buried organic matter (Pendleton et al. 2012, Arias-Ortiz et al. 2018). To better anticipate changes in seagrass ecosystems under future warming scenarios, it is critical to enhance our understanding of how seagrass ecosystems respond to heat stress.

Temperature effects on seagrass growth are complex and not fully clarified. It is well-known that increasing temperatures stimulate seagrass photosynthesis until reaching an optimum temperature threshold ($T_{th}$) (e.g. Marsh et al. 1986, Lee et al. 2007). Beyond this threshold, increasing temperatures cause thermal damage to the photosynthetic apparatus (Wahid et al. 2007, York et al. 2013), and the photosynthetic efficiency of the plant declines (e.g. Marsh et al. 1986, Abe et al. 2008, Niu et al. 2012). Respiration, however, increases more rapidly than photosynthesis with increasing temperature and continues to do so well past $T_{th}$ (Marsh et al. 1986, Staehr & Borum 2011). This metabolic imbalance leads to a carbon deficit within the plants, which results in impaired

*Corresponding author: acb4rk@virginia.edu



Publisher: Inter-Research · www.int-res.com

growth and loss of seagrass biomass (Moore & Short 2006, Lee et al. 2007, Collier et al. 2011, Ewers 2013). Therefore, it is no surprise that determining $T_{th}$ for seagrass species has been the focus of many studies aiming to better understand the impacts of heat stress on seagrasses (e.g. Nejrup & Pedersen 2008, Collier et al. 2011, Pedersen et al. 2016, Egea et al. 2019, Rasmusson et al. 2020).

Eelgrass *Zostera marina* is a widespread temperate seagrass species that is particularly at risk of local extinction at the southern edge of its distribution off the Mid-Atlantic coast (Koch & Orth 2003, Wilson & Lotze 2019), due to the expected increase in the frequency, duration, and intensity of extreme heating events throughout the 21st century (Frölicher et al. 2018, Oliver et al. 2019). The temperature threshold for *Z. marina* has been estimated between 25 and 30°C (Lee et al. 2007). Some studies have related $T_{th}$ to changes in eelgrass biomass or cover, taking advantage of large spatial scales (ecosystem-scale) and long time series (~10–40 yr) (Lefcheck et al. 2017, Richardson et al. 2018, Shields et al. 2019). However, the temporal resolution of seagrass cover or biomass data is often coarse (monthly to biennially), and the estimated $T_{th}$ may not accurately reflect the temperature at which seagrasses become physiologically stressed. Other studies aiming to determine this critical threshold do so by incubating leaf fragments (e.g. Marsh et al. 1986, Rasmusson et al. 2020) or whole shoots (Nejrup & Pedersen 2008) at discrete temperature intervals (often 2–5°C) and under controlled light conditions. Leaf fragments and whole shoots are typically incubated in the laboratory for a few hours and a few weeks, respectively. Photosynthetic rates and growth parameters such as new leaf production and leaf elongation are usually measured at the end of the experiment. These studies provide valuable insights into the thermal tolerance limits of seagrass plants but are difficult to translate to the ecosystem scale given that they are performed under controlled, static conditions and often exclude non-photosynthetic organs (roots and rhizomes) and other autotrophs and heterotrophs, which together contribute to whole-plant carbon balance and seagrass ecosystem response to heat stress.

To more realistically constrain $T_{th}$ for eelgrass ecosystems, it is essential to measure *in situ* eelgrass ecosystem metabolism under naturally varying environmental conditions. Our goal in this study was to determine $T_{th}$ of a vulnerable eelgrass meadow at the southern edge of the species' distribution. To do this, we relied on our substantial database of benthic oxygen ($O_2$) fluxes measured by aquatic eddy covariance (AEC; Berg et al. 2003) at the Virginia Coast Reserve (VCR) (Hume et al. 2011, Rheuban et al. 2014a,b, Berg et al. 2019, Berger et al. 2020, this study). Benthic $O_2$ fluxes are widely used as a proxy for ecosystem metabolism (e.g. Glud 2008, Rheuban et al. 2014b, Volaric et al. 2018, Berger et al. 2020, Berg et al. 2022), and this state-of-the-art *in situ* technique is well-suited for measuring instantaneous changes in seagrass ecosystem metabolism as a result of naturally fluctuating temperatures, as it is non-invasive (Lorrai et al. 2010) and measures benthic $O_2$ fluxes at a high temporal resolution (Rheuban & Berg 2013) over a 10–100 $m^2$ footprint (Berg et al. 2007), thus capturing whole-ecosystem processes. Preliminary data analyses of summer eelgrass ecosystem metabolism during cool days (temperatures <25°C, n = 6 days binned by hour-of-day) and hot days (afternoon temperatures >28°C, n = 7 days) revealed a strong negative effect of elevated temperatures on eelgrass ecosystem production (Fig. 1). This clear pattern motivated our further investigation into the threshold at which this negative effect occurs. To our knowledge, this is the first time a temperature stress threshold for eelgrass ecosystem production was determined from *in situ* and non-invasive metabolic measurements.

## 2. MATERIALS AND METHODS

### 2.1. Study site

The VCR Long-Term Ecological Research (VCR-LTER) site, located along the Atlantic side of the Delmarva Peninsula, is home to the largest successful eelgrass restoration project in the world (Orth & McGlathery 2012). This study took place in South Bay, which contains the largest of 4 previously restored eelgrass meadows at this site (~20 $km^2$ as of 2018, Orth et al. 2020; Fig. 2). Our measurements were conducted at 2 sites in the original restoration area of the meadow, a 7 $km^2$ region located just west of a barrier island and connected to the Atlantic Ocean by 2 inlets north and south of the meadow. This creates a low-energy hydrodynamic environment where light conditions are favorable to eelgrass growth (Lawson et al. 2007). Long-term data at the site also show relatively constant salinity and consistently high water quality due to the negligible freshwater inputs into the lagoons and limited human development around the VCR, resulting in low sediment and nutrient loading (Moore et al. 2012, Oreska et al.

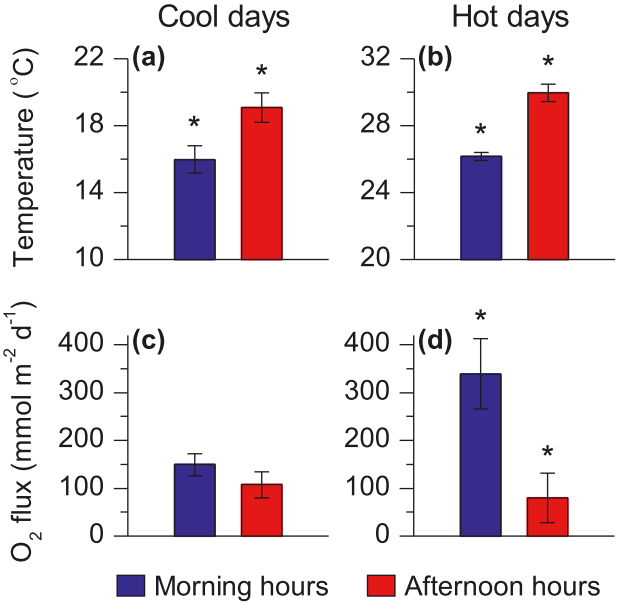


Fig. 1. Preliminary data analyses from aquatic eddy covariance measurements in South Bay show a negative effect of high temperatures on seagrass ecosystem metabolism. We compared (a,b) mean temperature and (c,d) associated oxygen ($O_2$) fluxes during 3 h in the morning and 3 h in the afternoon for a subset of 6 days on which (a,c) water temperatures were relatively cool (14–22°C) and 7 days on which (b,d) afternoon water temperatures exceeded the 28°C threshold proposed by Moore & Jarvis (2008). These bins were produced to have similar photosynthetically active radiation (PAR) levels in the morning and afternoon, to ensure that any observed differences in $O_2$ fluxes would not result from varying light conditions. Current velocity was also similar between morning and afternoon hours. Error bars are ±SE (n = 18 and 21 hours for cool days and hot days, respectively). Asterisks designate statistically significant differences between morning and afternoon hours (2-sample *t*-test, $p < 0.05$)

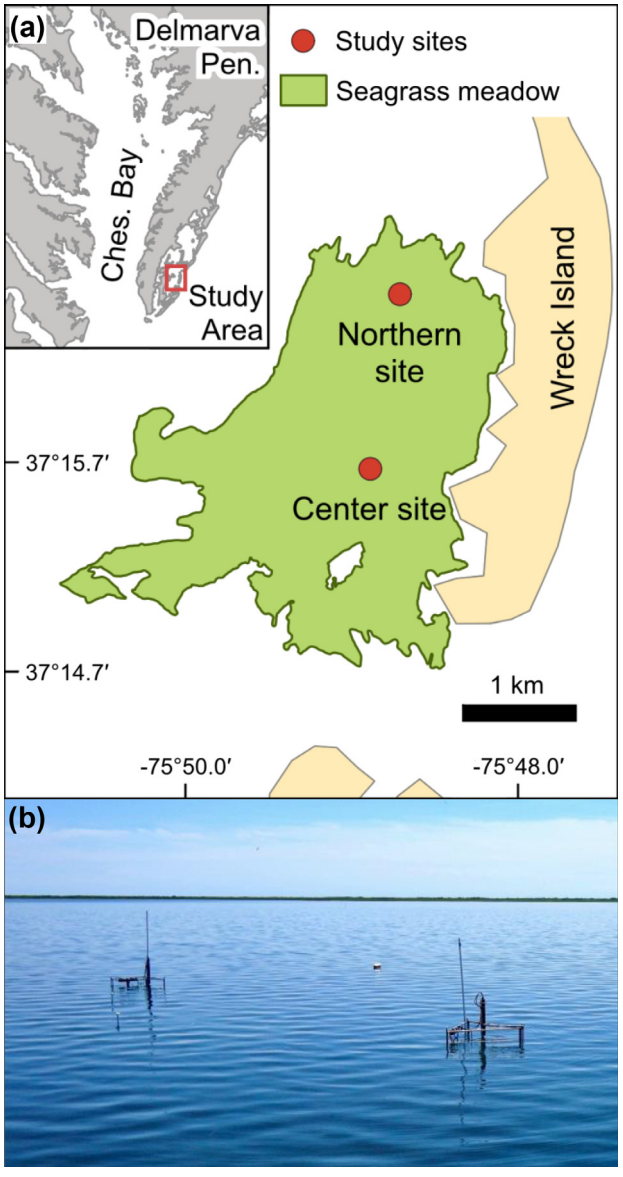


Fig. 2. (a) Study site locations in the South Bay eelgrass meadow at the Virginia Coast Reserve Long-Term Ecological Research site (VCR-LTER), on the Atlantic side of the Delmarva Peninsula (inset). (b) Aquatic eddy covariance systems deployed side-by-side in South Bay

2021). South Bay is shallow (mean water depth = 1.2 m) and experiences semi-diurnal tides with a tidal range of 1 m (Fagherazzi & Wiberg 2009). The eelgrass meadows of the VCR-LTER are growing close to the southern geographical limit for *Zostera marina* (Moore & Short 2006).

In June 2015, the VCR-LTER region experienced a marine heatwave, which led to a dramatic eelgrass die-off event in South Bay (Berger et al. 2020, Aoki et al. 2021). Long-term eelgrass monitoring efforts at the 6 original restoration plots at the center of South Bay captured this ~90% decline in eelgrass shoot density and its slow recovery in the following years (Berger et al. 2020, Aoki et al. 2021).

Eelgrass ecosystem metabolism was measured by AEC at 2 sites in South Bay: one in the northern part of the meadow ('northern site': 37° 16′ 34.2″ N, 75° 48′ 44.4″ W) and one in the center of the meadow ('center site': 37° 15′ 43.6″ N, 75° 48′ 54.6″ W) (Fig. 2). The center site is one of the original restoration plots and has been part of a long-term study (2007–present) on eelgrass ecosystem metabolism measured by AEC (Hume et al. 2011, Rheuban et al. 2014a,b, Berg et al. 2019, Berger et al. 2020). In summer 2019, the northern site was added to our study design, and we alternated eelgrass ecosystem metabolism measurements between both sites throughout the summer.

### 2.2. Eelgrass metabolism measurements by aquatic eddy covariance

We applied the AEC technique (Berg et al. 2003) to measure eelgrass ecosystem metabolism as described in detail by Berger et al. (2020). Briefly, this technique uses high-resolution (16–64 Hz) measurements of dissolved oxygen and current velocity field ($x$, $y$, $z$) to derive *in situ* benthic $O_2$ fluxes over a 10–100 $m^2$ footprint, thus capturing ecosystem-scale processes under naturally varying conditions (e.g. light, flow, and temperature). The oxygen and velocity sensors are mounted on a thin, stainless steel frame designed to minimize disturbances of the natural flow (Berg & Huettel 2008).

In this study, we used a mix of previously published (Berg et al. 2019, Berger et al. 2020) and new benthic flux data, focusing on the spring and summer months between 2014 and 2018 (n = 60 days). During summer 2019, we measured benthic fluxes for 3–7 consecutive days (usually 1 to 4 deployments, each 24–48 h in duration), alternating between the center and northern site (Fig. 2), totaling 45 days of data over the summer. For this new sampling period, we used a RINKO-EC micro planar optode (JFE Advantech) (Berg et al. 2016) to measure dissolved oxygen, as opposed to the Clark-Type microelectrodes (Unisense) used through 2018. The RINKO-EC sensor was considerably less fragile, thus ensuring a significantly higher deployment success rate. The sensor was placed 1.5 cm away from the edge of the velocity sensor's measuring volume, which was set at 30 cm above the seafloor. To account for the time lag between velocity and oxygen concentration measurements resulting from this distance, we applied a time-shift correction that maximized the covariance between fluctuations in $O_2$ concentration and vertical velocity over a 0–2 s period. Because of its tip size (8 mm), the RINKO-EC sensor can potentially interfere with the velocity measurements. We therefore deployed 2 AEC systems side-by-side, facing in opposite directions to measure benthic $O_2$ fluxes during flood tide and ebb tide, respectively (Fig. 2b). This ensured maximum measurement accuracy throughout the tidal cycle. The systems were deployed 10 m apart so that their footprints would not overlap. When processing the data collected by each system, we excluded data collected while the main current direction came from behind the sensor. During slack tide, we treated data on a case-by-case basis, often averaging the fluxes from both systems.

All AEC deployments also produced water depth measurements and coincided with measurements of photosynthetically active radiation (PAR) and water temperature. We used 2π PAR loggers (Odyssey) to measure PAR at 5 min intervals and miniDOT© (PME) optodes (accuracy ±0.1°C) to measure dissolved oxygen concentration and temperature at 1 min intervals. Both sensors were deployed at the top of the canopy, 30 cm above the sediment surface.

Differences in available light (PAR), water depth, and current speed between the center and northern sites during summer 2019 were assessed using 2-sample $t$-tests (significance level: 0.05) in the software program R (version 3.4.2; R Core Team 2017). Prior to conducting these $t$-tests, we screened our data for outliers (via visual inspection of boxplots and Cleveland dot plots) and ensured they met the assumptions of normality (through visual inspection of frequency distributions and Q–Q plots) and homogeneity of variances (by visually inspecting frequency distributions and employing Bartlett's test). Only daytime (non-zero) PAR data were included in these tests.

### 2.3. Identifying the temperature stress threshold

To determine the temperature threshold for heat stress ($T_{th}$) of the South Bay eelgrass meadow, we first identified subsets in our *in situ* hourly $O_2$ flux data where the range of temperatures during individual days was sufficiently large (~25–31°C) to capture the effects of increasing temperatures on eelgrass ecosystem metabolism and overlap with the 28°C threshold proposed by Moore & Jarvis (2008). We identified 5 such subsets from June 2015, 2019, and July 2019, each containing 36–89 h of continuous data. Hourly data in each subset were binned by hour of day to produce representative diel cycles. We also combined data from all subsets (n = 356 h = ~15 d) into one 24 h cycle to average over differences in sampling time and location and to represent an average day of heat stress in the meadow.

To identify the temperature threshold at which negative impacts on eelgrass ecosystem production occurred, we fit our $O_2$ flux data using a non-linear multivariate modeling approach using PAR, temperature, and hour of day as explanatory variables. Under non-stressful temperatures, our model simply described a typical photosynthesis–irradiance (P–I) relationship based on the function proposed by Jassby & Platt (1976) and previously used on our AEC data (Berg et al. 2019) (Fig. 3a,d):

$$\text{Benthic } O_2 \text{ flux} = P_m \times \tanh\frac{I}{I_k} + R \quad (1)$$

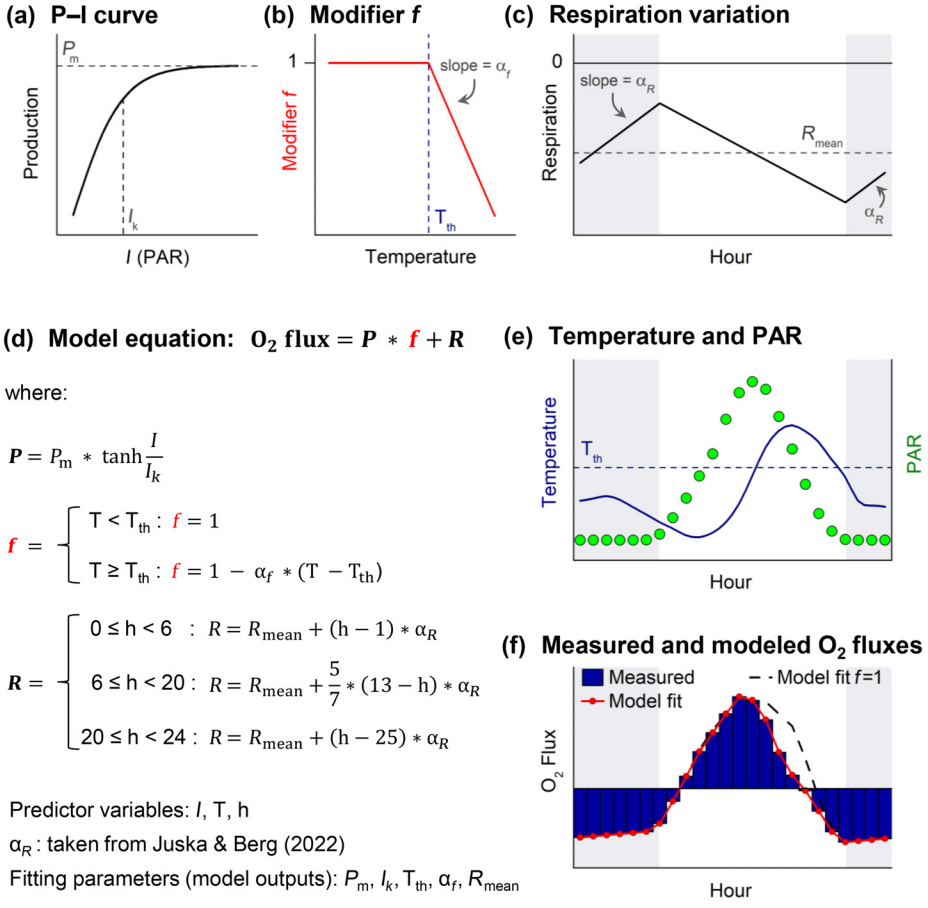


Fig. 3. Conceptual representation of the model used to determine the temperature threshold ($T_{th}$) above which eelgrass ecosystem production is negatively affected. The model equation (d) is based on a typical photosynthesis – irradiance (P – I) curve (a) modified by a factor $f$ (b), which is equal to 1 when temperature $<T_{th}$ and is <1 when temperature $\geq T_{th}$. (c) In this model, $R$ decreased linearly at a rate $\alpha_R$ = 5.11 mmol $O_2$ $m^{-2}$ $h^{-1}$ (Juska & Berg 2022) during nighttime hours (see Section 2.3 for details), and increased during the day by a rate of $-\alpha_R 5/7$ (5/7 being the ratio of nighttime to daytime hours). The fitting parameters were $P_m$ (maximum net photosynthetic rate); $I_k$ (light saturation constant); $T_{th}$ (temperature threshold); $\alpha_f$ (constant); and $R_{mean}$ (average respiration). $I$ (PAR), temperature, and $O_2$ fluxes were measured data. (e,f) An ideal set of hourly temperature (blue line), PAR (green dots), and $O_2$ fluxes (blue bars). Positive $O_2$ fluxes represent a release of oxygen (net photosynthesis), and negative $O_2$ fluxes represent oxygen uptake (respiration). Red line: $O_2$ fluxes predicted by our model. Dashed line: $O_2$ fluxes predicted by the P – I relationship without the modifier ($f$ = 1)

where $P_m$ is the maximum net photosynthetic rate, $I$ is available light at canopy height (PAR measurement), $I_k$ is the light saturation constant, and $R$ is respiration. In our model, the underlying P – I relationship accounted for variations in $R$ throughout the diel cycle that result from the production of highly labile compounds produced during the day and consumed at night (Fig. 3d), with $R$ decreasing linearly at a rate $\alpha_R$ = 5.11 mmol $O_2$ $m^{-2}$ $h^{-1}$ during the night and increasing by a rate of $-\alpha_R 5/7$ throughout the day (5/7 being the ratio between nighttime and daytime hours) (Juska & Berg 2022). This rate was determined from 2115 h of summer $O_2$ flux data measured by AEC at our same study site in South Bay (Juska & Berg 2022). The significantly smaller number of hours used in this study (n = 356) prohibited us from including $\alpha_R$ as a fitting parameter in our model. In previous studies, the effects of light and the production and consumption of labile compounds account for 99% of the variance in $O_2$ fluxes under non-stressful thermal conditions (Juska & Berg 2022). In this study, we therefore deemed the effects of current velocity on $O_2$ fluxes to be insignificant compared to the other drivers, particularly as our data were averaged over several days (Hume et al. 2011, Juska & Berg 2022).

Deviations of net photosynthesis measurements from this traditional P – I relationship (Fig. 3f) can therefore be primarily attributed to the effects of temperature threshold exceedance. To account for the drop in production due to heat stress, we included a

factor $f$ in our model (Fig. 3b) that attenuated the aforementioned P–I relationship when temperatures exceeded $T_{th}$ (Fig. 3). For temperatures below $T_{th}$, $f$ was equal to 1 (no attenuation). In other words, our model identified the temperature $T_{th}$ beyond which net photosynthesis deviated from what would be expected solely based on light levels (Fig. 3c,e).

This fitting model was written in Fortran and run on each of our 5 subsets of hourly data and the combination of all 356 h of data. The model outputs were $T_{th}$, a constant $\alpha_f$, $R_{mean}$ (used in R calculations), $P_m$, and $I_k$ (Fig. 3d). The program performed on average $16.8 \times 10^8$ iterations each run to find the best combination of parameter values to fit our measured $O_2$ fluxes. Because our model is nonlinear, all reported $R^2$ values in our results come from a linear regression performed between the observed and predicted $O_2$ fluxes.

## 3. RESULTS

### 3.1. Site characteristics

Water depth and light availability (PAR) were not significantly different between the center and northern sites: with only a difference of 6 cm in water depth (2-sample $t$-test, $t_{465} = 1.52$, $p = 0.13$, $n = 500$ h), and 150 µmol $m^{-2}$ $s^{-1}$ in PAR, which represents ~ 7% of maximum daytime PAR at these sites (2-sample $t$-test, $t_{78} = 1.11$, $p = 0.27$, $n = 80$ h). PAR varied from 0 to ~2000 µmol $m^{-2}$ $s^{-1}$, the latter being measured at midday during low tide. Current speeds at the center site ranged from 0.4 to 9.8 cm $s^{-1}$ (mean: 2.8 cm $s^{-1}$), and those at the northern site ranged from 0.4 to 13.1 cm $s^{-1}$ (mean: 4.9 cm $s^{-1}$). This average difference of 2.1 cm $s^{-1}$ was statistically significant (2-sample $t$-test, $t_{403} = -9.57$, $p < 0.05$, $n = 500$ hours).

### 3.2. Temperature threshold

Our model identified 28.6°C as the temperature threshold beyond which negative impacts on net ecosystem photosynthesis occurred (Table 1). Each model run fit our data extremely well ($R^2 = 0.92–0.99$) and produced temperature threshold estimates between 27.8 and 29.5°C, diverging only ±3% from the average of 28.6°C (Table 1). The model was only run on 5 data subsets; therefore, no clear patterns in $T_{th}$ estimates between sites or sampling times could be identified. $P_m$ was much higher at the northern site (1282 mmol $O_2$ $m^{-2}$ $d^{-1}$) than at the center site (540 mmol $O_2$ $m^{-2}$ $d^{-1}$), and the light saturation constant ($I_k$) increased between June (mean $I_k$ = 982 µmol $m^{-2}$ $s^{-1}$) and July (mean $I_k$ = 1727 µmol $m^{-2}$ $s^{-1}$) (Table 1).

### 3.3. Effects of temperature threshold exceedance on eelgrass production

During days of heat stress, we observed a notable drop in net photosynthesis compared to what would be expected under the measured light levels. Fig. 4 displays a side-by-side comparison of our measured and predicted $O_2$ fluxes under cool conditions (Fig. 4a,c; temperatures averaging 15–18°C over a 24 h cycle obtained from 429 h of data from April 2015, 2017, and 2018 binned by hour of day) and heat-stressed conditions (Fig. 4b,d; temperatures averaging 26–30°C, full composite of 356 h of data — see Section 2.3). While a P–I relationship (modified for diel $R$ variability as in Juska & Berg 2022) accurately predicted oxygen fluxes during cool days ($R^2 = 0.99$), it would have overestimated afternoon fluxes during hot days, as shown in Fig. 4b (dashed line) where the modifier $f$ in our model (Fig. 3) was set to a fixed value of 1. When our model took into account the existence of a temperature threshold, the decrease in net photosynthesis as a result of heat stress was well predicted ($R^2 = 0.99$, Fig. 4b). In the hour following threshold exceedance (hour 14.5, Fig. 4b), our model predicted an $O_2$ flux 24% lower than what a simple P–I function would have predicted (model $O_2$ flux = 299 mmol $O_2$ $m^{-2}$ $d^{-1}$ vs. P–I $O_2$ flux = 394 mmol $O_2$ $m^{-2}$ $d^{-1}$). The largest difference in $O_2$ flux predictions occurred at hour 16.5, where the predicted $O_2$ flux under heat

Table 1. Model results from 6 runs on aquatic eddy covariance data from June 2015, 2019, and July 2019 at the northern and center sites (total = 356 h). $T_{th}$ = temperature threshold (°C), $\alpha_f$ = parameter where $f = 1 - \alpha_f (T - T_{th})$, $R_{mean}$ = average respiration (mmol $O_2$ $m^{-2}$ $d^{-1}$), $P_m$ = maximum photosynthetic rate (mmol $O_2$ $m^{-2}$ $d^{-1}$), and $I_k$ = light saturation constant (µmol $m^{-2}$ $s^{-1}$). N is given in hours, and $R^2$ is the coefficient of determination, calculated from a linear regression between observed and predicted $O_2$ fluxes

| Warm period | Site | $T_{th}$ | $\alpha_f$ | $R_{mean}$ | $P_m$ | $I_k$ | $R^2$ | N |
|---|---|---|---|---|---|---|---|---|
| All data | Both | 28.6 | 0.2 | −242 | 684 | 1161 | 0.99 | 356 |
| June 2015 | Center | 29.1 | 0.7 | −127 | 338 | 1002 | 0.97 | 84 |
| June 2019 | Center | 28.1 | 0.05 | −159 | 442 | 961 | 0.96 | 36 |
| July 2019 | Northern | 27.9 | 0.2 | −336 | 825 | 1130 | 0.95 | 80 |
| July 2019 | Center | 28.8 | 0.3 | −235 | 841 | 1718 | 0.92 | 89 |
| Late July 2019 | Northern | 29.3 | 0.2 | −294 | 1738 | 2334 | 0.92 | 67 |
| Average | | 28.6 | | | | | | |

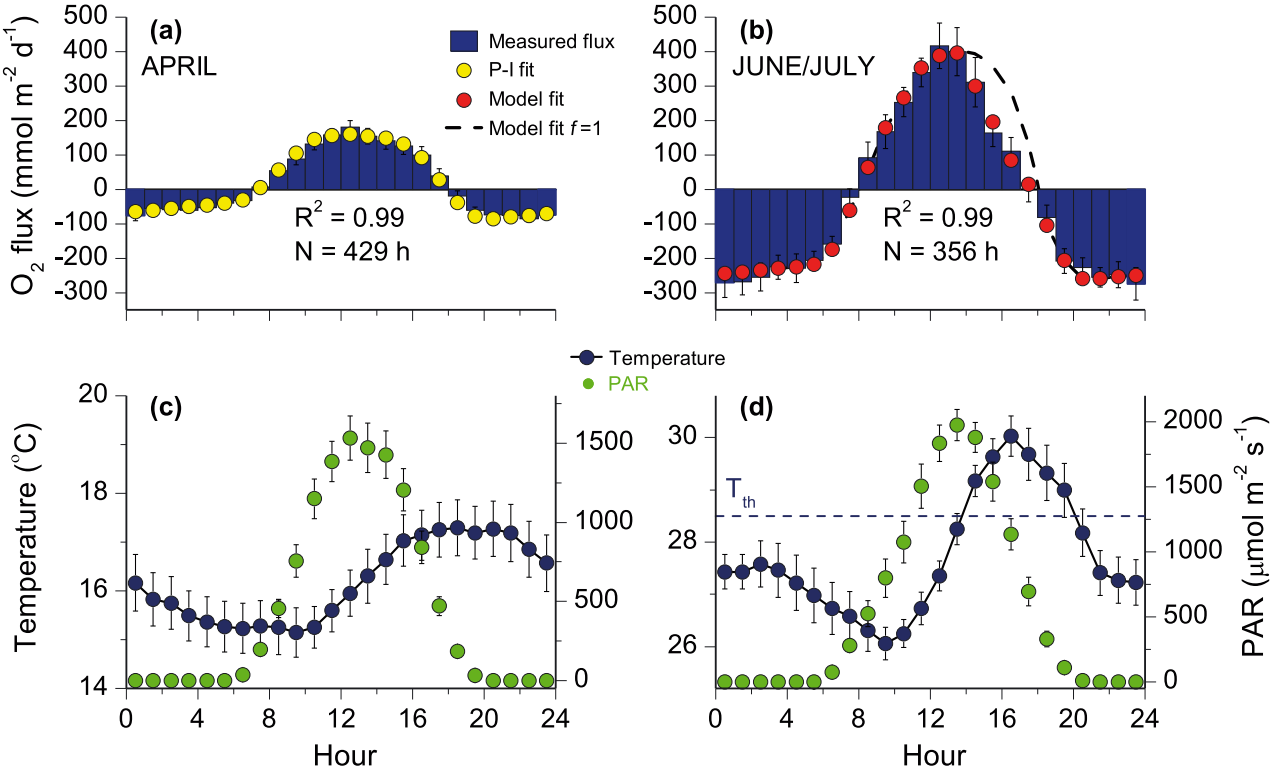


Fig. 4. Oxygen flux (blue bars), temperature (blue dots), and PAR (green dots) measured in (a,c) April 2015, 2017, and 2018 and (b,d) June 2015, 2019, and July 2019, binned by hour of day (n = 429 and 356 hours binned, respectively). Temperatures in April ranged from 15.1 to 17.3°C, and summer temperatures ranged from 26.1 to 30.0°C. Yellow dots in (a): oxygen fluxes predicted by a P—I relationship. Red dots in (b): oxygen fluxes predicted by our model. Dashed line in (b): predicted oxygen fluxes by our model if the effects of temperature were not accounted for (*f* set to 1). Error bars are ± SE

stress was 70% lower than that predicted without accounting for temperature. On average, our model predicted afternoon fluxes ~50% lower than what a simple P—I function would have yielded. For our binned day (Fig. 4b), this difference accounts for a cumulative 574 mmol $O_2$ $m^{-2}$ $d^{-1}$.

## 4. DISCUSSION

A key aspect in understanding the response of seagrass ecosystems to heat stress is knowing the temperature threshold above which seagrass ecosystem production is negatively affected. A number of studies have investigated this threshold for seagrass plants (e.g. Marsh et al. 1986, Hammer et al. 2018, Rasmusson et al. 2020) by relying on *ex situ* approaches that are difficult to extrapolate to the ecosystem scale. Here we combined a non-linear multivariate model fitting with our extensive database of hourly benthic $O_2$ fluxes measured *in situ* by AEC under naturally varying field conditions to identify 28.6°C as the thermal tolerance threshold for a local *Zostera marina* meadow. Exceeding this threshold resulted in a 20—70% decrease in net photosynthesis, which has implications for the carbon balance of eelgrass meadows and their vulnerability to warming oceans. The close match observed between our data set and model predictions (Fig. 4, Table 1) highlights the effectiveness of integrating continuous environmental and ecosystem metabolism data to determine a precise temperature threshold.

### 4.1. Temperature threshold

Our temperature threshold estimate of 28.6°C agrees well with several other studies conducted on *Z. marina* populations near the species' thermal distribution boundary (Moore & Jarvis 2008, Carr et al. 2012, Shields et al. 2018). Carr et al. (2012) found a similar threshold of 28.5°C using a vegetation growth model for eelgrass at the VCR, while Moore & Jarvis (2008) and Shields et al. (2018) related eelgrass declines in the Chesapeake Bay to temperatures above 28°C. Other studies identified a range for $T_{th}$ between

25 and 30°C (e.g. Marsh et al. 1986, Hammer et al. 2018, Rasmusson et al. 2020). However, these latter studies involved *ex situ* incubations at discrete and coarse temperature intervals (e.g. from 25 or 27 to 30°C) and were therefore unable to identify a precise temperature threshold (e.g. Hammer et al. 2018 estimated that $T_{th}$ fell between 26 and 30°C).

Globally, however, $T_{th}$ estimates for *Z. marina* vary between 16 and 35°C, and average ~20°C (Lee et al. 2007). This variation is largely attributed to latitude. Eelgrass populations growing in Massachusetts (USA), Denmark, and Korea have shown decreased photosynthesis and growth at temperatures exceeding 20°C (Marsh et al. 1986, Lee et al. 2005, Nejrup & Pedersen 2008). In China, negative temperature effects were observed above 16–20°C (Niu et al. 2012). These geographical differences in thermal stress tolerance suggest there are eelgrass 'ecotypes,' i.e. different populations that are genetically adapted to the environmental conditions where they are growing (Nejrup & Pedersen 2008). Eelgrass populations adapted to lower temperatures are therefore likely vulnerable to temperatures exceeding a lower temperature threshold compared to the 28.6°C threshold found in this study for a population near the thermal boundary of the species' geographic range. In addition, eelgrasses have been shown to acclimate to seasonal temperature variations and become more resilient to subsequent stressful events (Staehr & Borum 2011, Jueterbock et al. 2020, Nguyen et al. 2020). Some variability in $T_{th}$ estimates is therefore possible depending on the timing of the study and chosen eelgrass populations. Although based on only a few data subsets, our results seem to support the notion that eelgrass ecosystems can tolerate slightly higher temperatures after previous exposure to temperatures exceeding $T_{th}$, as seen in the slight increase in $T_{th}$ from June to July 2019 at the center site ($T_{th}$ increase from 28.1 to 28.8°C) and from early to late July 2019 at the northern site ($T_{th}$ increase from 27.9 to 29.3°C) (Table1). The center and northern sites experience different levels of thermal stress and cooling due to their location in the meadow relative to the northern inlet (Berger et al. 2024, this volume). While we did not find a clear pattern of $T_{th}$ between sites (Table 1), it is possible that with more data, we would be able to identify a lower $T_{th}$ for the less heat-stressed northern site compared to the center site. Out of the 114 days of summer data we have collected since 2007 (Hume et al. 2011, Rheuban et al. 2014b, Berg et al. 2019, Berger et al. 2020, this study), only ~14 met the criteria for this type of analysis, as we had to find days with a relatively large temperature range (~25–31°C) somewhat centered around 28°C.

Temperature threshold estimates may also differ for eelgrass populations dealing with additional stressors such as turbidity, as eelgrass light requirements to maintain a positive carbon balance have been shown to increase with increasing temperatures (Moore et al. 2012). This is in line with our results, as $I_k$ increased between June and July (Table 1). Consequently, in deeper meadows or under more turbid conditions, eelgrasses stressed by low-light conditions might be more sensitive to an increase in temperature, and therefore have a lower threshold for thermal stress.

The large range in published temperature threshold estimates may also result from different methodological approaches. Lab incubations are conducted under controlled and static environmental conditions (namely PAR, e.g. Abe et al. 2008) and for different lengths of time — from 15–30 min (Marsh et al. 1986) to 6 wk (Nejrup & Pedersen 2008). Some may also only incubate leaf fragments (e.g. Marsh et al. 1986, Dennison 1987, Rasmusson et al. 2020) instead of whole shoots. Consequent metabolism measurements may therefore be overestimated as they exclude the respiration rates of seagrass roots and rhizomes, which are important to the carbon balance of the plant (Pregnall et al. 1984). While whole-shoot incubations include below-ground biomass (e.g. Nejrup & Pedersen 2008), it may still be difficult to extrapolate results to represent ecosystem-scale processes where intact shoots rooted in the sediment are growing under naturally fluctuating environmental conditions. It should be noted that these laboratory incubation studies have primarily focused on determining the temperature threshold for eelgrass leaves or whole plants, rather than examining the response of an entire ecosystem or community exposed to naturally varying environmental conditions, as is the central focus of our study.

### 4.2. Assumptions and limitations of this study

In this study, we used eelgrass ecosystem metabolism data to determine a temperature threshold for eelgrass physiological stress at the meadow scale. We suggest that prolonged exposure to temperatures above this threshold could lead to a decline in eelgrass biomass. We base this on the premise that eelgrass plants dominate benthic metabolism at our study site, which has been supported by previous AEC studies at this site (Rheuban et al. 2014a,b, Berg et al. 2019, Berger et al. 2020). Our confidence in our

findings is further supported by the agreement of our threshold (28.6°C) with the one proposed by Carr et al. (2012) (28.5°C), which was based on an eelgrass growth model incorporating site-based parameters such as shoot density, leaf length, and above-and below-ground biomass. We caution, however, that applying the approach used in this study to a meadow where seagrass is not the driver of ecosystem-scale processes could lead to inaccurate assessments of ecosystem temperature stress. In such a case, the estimated temperature threshold may not accurately reflect the temperature above which sustained warming might trigger a decline in seagrass biomass. Indeed, some studies have shown that other components of the seagrass meadow community (i.e. benthic microalgae, phytoplankton) contribute substantially to whole-ecosystem metabolism. For example, Murray & Wetzel (1987) estimated in an eelgrass meadow that both sediments and phytoplankton contributed to gross primary production (10–25 and 10–48%, respectively) and respiration (8–23 and 9–73%, respectively). Similarly, in a subtropical seagrass meadow, Cox et al. (2020) found that diatoms accounted for 71–83% of benthic metabolism. This underscores the importance of considering ecosystem-specific dynamics when determining temperature thresholds.

### 4.3. Effects of thermal stress on eelgrass metabolism

Our results showed a strong negative effect of temperature threshold exceedance on eelgrass meadow production (Fig. 4), as reflected in the reduction in net photosynthesis of up to 70% that coincided with peak temperature during an average June/July 24 h cycle (Fig. 4b,d). On average, net photosynthesis was reduced by 50% compared to photosynthetic rates under the same light levels in the absence of heat stress (Fig. 3b). Nejrup & Pedersen (2008) found a comparable decrease in eelgrass photosynthetic rates above 25–30°C. This decline in net $O_2$ flux was attributed to both the inhibition of photosynthesis at high temperatures and increased respiration. Given a whole-plant respiratory Q10 value of 1.5 for *Z. marina* for this temperature range (i.e. a 1.5-fold increase in respiration for every 10°C increase, Rasmusson et al. 2019), respiration would have only increased by 7% (on the order of 17 mmol $O_2$ $m^{-2}$ $d^{-1}$ based on $R_{mean}$) as temperatures reached their maximum of 30°C (Fig. 4d). This increase is almost negligible compared to the 172 mmol $O_2$ $m^{-2}$ $d^{-1}$ difference in $O_2$ fluxes under heat-stressed and non-stressed conditions (Fig. 4b), which suggests that the observed decline in seagrass ecosystem metabolism is primarily due to inhibition of photosynthesis when temperatures exceed $T_{th}$.

A reduction in photosynthesis at temperatures above $T_{th}$ has negative implications for the carbon balance of eelgrass meadows. When we calculated daily metabolic rates (as defined by Hume et al. 2011, Rheuban et al. 2014b, and Berger et al. 2020) from our averaged 24 h cycle (N = 356 h, Fig. 4b), we found that gross primary production (GPP) was ~5% lower compared to that calculated from fluxes predicted by a simple P–I function that excluded heat stress (dashed line in Fig. 4b) (GPP = 224 vs. 236 mmol $O_2$ $m^{-2}$ $d^{-1}$). Concurrently, daily respiration was ~5% higher than that calculated in the absence of heat stress (−253 vs. −242 mmol $O_2$ $m^{-2}$ $d^{-1}$). While these differences seem relatively small, they were enough to result in a negative carbon balance (net ecosystem metabolism = −30 mmol $O_2$ $m^{-2}$ $d^{-1}$), when in the absence of heat stress, the meadow would have been closer to metabolic balance (net ecosystem metabolism = −6 mmol $O_2$ $m^{-2}$ $d^{-1}$).

Carbon balance plays a critical role in the response of eelgrass meadows to stress. Under high-temperature conditions, seagrass carbon acquisition is reduced, and the plants allocate more resources to maintenance or repair processes to withstand heat stress, rather than allocating resources to growth, reproduction, and storage (Burke et al. 1996, Sokolova 2013, Moreno-Marín et al. 2018). This hinders seagrass survival and resilience through reduced growth and increased mortality (Marsh et al. 1986, Moreno-Marín et al. 2018) as well as through decreased reproductive performance (Qin et al. 2020, Johnson et al. 2021). This would result in a reduced ability for eelgrasses to maintain their habitats and genetic diversity, which threatens their resilience and potential for adapting to climate change (Ehlers et al. 2008).

### 4.4. Future projections for *Z. marina* meadows

Eelgrass meadows at the VCR are growing at the southern thermal boundary of the species' geographic range (Moore & Jarvis 2008), where summertime water temperatures often exceed their 28.6°C thermal tolerance threshold. This highlights the vulnerability of these ecosystems to the projected increase in global temperatures and extreme heating events such as marine heatwaves (Frölicher et al. 2018, Oliver et al. 2019), despite their ability to acclimate and adapt to elevated temperatures in the short term (Staehr &

Borum 2011). It is not yet clear how this adaptation to heat stress may persist in the long term or be conferred to subsequent generations (Jueterbock et al. 2020, Nguyen et al. 2020). Future warming scenarios project an average shift of the southern eelgrass range by 1.4–6.5° N by 2100, which would likely result in a complete loss of eelgrass in the VCR and Chesapeake Bay region (Wilson & Lotze 2019). These regions could see a community shift towards more heat-tolerant seagrass species, as some regions of the Chesapeake Bay have experienced a change in the relative abundance of *Z. marina* and the more heat-tolerant *Ruppia maritima* (Moore et al. 2014, Richardson et al. 2018, Shields et al. 2019). This change in favor of *R. maritima* over *Z. marina* has been largely attributed to rising temperatures (Richardson et al. 2018, Shields et al. 2019). The consequences of such community shifts or eelgrass loss on the ecosystem services of eelgrass meadows, particularly carbon storage, are unknown and may be extreme. For example, the marine heatwave that led to the eelgrass die-off at the VCR in 2015 led to a 20% loss of previously-stored sediment carbon that had accumulated over ~15 yr (Aoki et al. 2021). The ongoing increase in ocean temperatures and severe heating events call for appropriate metrics to describe the relationships between these short-term, high-stress events and their long-term impacts on marine ecosystems.

*Acknowledgements*. This work was supported by the National Science Foundation (Virginia Coast Reserve Long Term Ecological Research grant, DEB-1237733 and DEB-1832221). We thank the staff at the University of Virginia's Coastal Research Center for their field and lab assistance, as well as REU students for their help in data collection.

## LITERATURE CITED

Abe M, Kurashima A, Maegawa M (2008) High water-temperature tolerance in photosynthetic activity of *Zostera marina* seedlings from Ise Bay, Mie Prefecture, central Japan. Fish Sci 74:1017–1023

Aoki LR, McGlathery KJ, Wiberg PL, Oreska MPJ, Berger AC, Berg P, Orth RJ (2021) Seagrass recovery following marine heat wave influences sediment carbon stocks. Front Mar Sci 7:576784

Arias-Ortiz A, Serrano O, Masqué P, Lavery PS and others (2018) A marine heatwave drives massive losses from the world's largest seagrass carbon stocks. Nat Clim Change 8:338–344

Beck MW, Heck KL, Able KW, Childers DL and others (2001) The identification, conservation, and management of estuarine and marine nurseries for fish and invertebrates. BioScience 51:633–641

Berg P, Huettel M (2008) Integrated benthic exchange dynamics. Oceanography 21:164–167

Berg P, Røy H, Janssen F, Meyer V, Jørgensen BB, Huettel M, De Beer D (2003) Oxygen uptake by aquatic sediments measured with a novel non-invasive eddy-correlation technique. Mar Ecol Prog Ser 261:75–83

Berg P, Røy H, Wiberg PL (2007) Eddy correlation flux measurements: the sediment surface area that contributes to the flux. Limnol Oceanogr 52:1672–1684

Berg P, Koopmans DJ, Huettel M, Li H, Mori K, Wüest A (2016) A new robust oxygen-temperature sensor for aquatic eddy covariance measurements. Limnol Oceanogr Methods 14:151–167

Berg P, Delgard ML, Polsenaere P, McGlathery KJ, Doney SC, Berger AC (2019) Dynamics of benthic metabolism, $O_2$, and $pCO_2$ in a temperate seagrass meadow. Limnol Oceanogr 64:2586–2604

Berg P, Huettel M, Glud RN, Reimers CE, Attard KM (2022) Aquatic eddy covariance: the method and its contributions to defining oxygen and carbon fluxes in marine environments. Annu Rev Mar Sci 14:431–455

Berger AC, Berg P, McGlathery KJ, Delgard ML (2020) Long-term trends and resilience of seagrass metabolism: a decadal aquatic eddy covariance study. Limnol Oceanogr 65: 1423–1438

Berger AC, Berg P, McGlathery KJ, Aoki LR, Kerns K (2024) Eelgrass meadow response to heat stress. II. Impacts of ocean warming and marine heatwaves measured by novel metrics. Mar Ecol Prog Ser 736:

ditions, fetch, and water levels on wave-generated shear stresses in shallow intertidal basins. J Geophys Res Earth Surf 114:F03022
Fourqurean JW, Duarte CM, Kennedy HA, Marbà N and others (2012) Seagrass ecosystems as a globally significant carbon stock. Nat Geosci 5:505–509
Frölicher TL, Fischer EM, Gruber N (2018) Marine heatwaves under global warming. Nature 560:360–364
Glud RN (2008) Oxygen dynamics of marine sediments. Mar Biol Res 4:243–289
Hammer KJ, Borum J, Hasler-Sheetal H, Shields EC, Sand-Jensen K, Moore KA (2018) High temperatures cause reduced growth, plant death and metabolic changes in eelgrass *Zostera marina.* Mar Ecol Prog Ser 604:121–132
Hume AC, Berg P, McGlathery KJ (2011) Dissolved oxygen fluxes and ecosystem metabolism in an eelgrass (*Zostera marina*) meadow measured with the eddy correlation technique. Limnol Oceanogr 56:86–96
Jassby AD, Platt T (1976) Mathematical formulation of the relationship photosynthesis and light for phytoplankton. Limnol Oceanogr 21:540–547
Johnson AJ, Shields EC, Kendrick GA, Orth RJ (2021) Recovery dynamics of the seagrass *Zostera marina* following mass mortalities from two extreme climatic events. Estuar Coasts 44:535–544
Jueterbock A, Boström C, Coyer JA, Olsen JL and others (2020) The seagrass methylome is associated with variation in photosynthetic performance among clonal shoots. Front Plant Sci 11:571646
Juska I, Berg P (2022) Variation in seagrass meadow respiration measured by aquatic eddy covariance. Limnol Oceanogr Lett 7:410–418
Koch EW, Orth RJ (2003) The Mid-Atlantic coast of the United States. In: Green EP, Short FT (eds) World atlas of seagrasses. University of California Press, Berkeley, CA, p 216–223
Koch EW, Barbier EB, Silliman BR, Reed DJ and others (2009) Non-linearity in ecosystem services: temporal and spatial variability in coastal protection. Front Ecol Environ 7: 29–37
Lawson SE, Wiberg PL, McGlathery KJ, Fugate DC (2007) Wind-driven sediment suspension controls light availability in a shallow coastal lagoon. Estuar Coasts 30: 102–112
Lee KS, Park SR, Kim JB (2005) Production dynamics of the eelgrass, *Zostera marina* in two bay systems on the south coast of the Korean peninsula. Mar Biol 147:1091–1108
Lee KS, Park SR, Kim YK (2007) Effects of irradiance, temperature, and nutrients on growth dynamics of seagrasses: a review. J Exp Mar Biol Ecol 350:144–175
Lefcheck JS, Wilcox DJ, Murphy RR, Marion SR, Orth RJ (2017) Multiple stressors threaten the imperiled coastal foundation species eelgrass (*Zostera marina*) in Chesapeake Bay, USA. Glob Change Biol 23:3474–3483
Lorrai C, McGinnis DF, Berg P, Brand A, Wüest A (2010) Application of oxygen eddy correlation in aquatic systems. J Atmos Ocean Technol 27:1533–1546
Marbá N, Duarte CM (2010) Mediterranean warming triggers seagrass (*Posidonia oceanica*) shoot mortality. Glob Change Biol 16:2366–2375
Marsh JA Jr, Dennison WC, Alberte RS (1986) Effects of temperature on photosynthesis and respiration in eelgrass (*Zostera marina* L.). J Exp Mar Biol Ecol 101:257–267
Moore KA, Jarvis JC (2008) Environmental factors affecting recent summertime eelgrass diebacks in the lower Chesapeake Bay: implications for long-term persistence. J Coast Res 2008:135–147
Moore KA, Short FT (2006) *Zostera*: biology, ecology, and management. In: Larkum R, Orth RJ, Duarte CM (eds) Seagrasses: biology, ecology and conservation. Springer, Dordrecht, p 361–386
Moore KA, Shields EC, Parrish DB, Orth RJ (2012) Eelgrass survival in two contrasting systems: role of turbidity and summer water temperatures. Mar Ecol Prog Ser 448: 247–258
Moore KA, Shields EC, Parrish DB (2014) Impacts of varying estuarine temperature and light conditions on *Zostera marina* (eelgrass) and its interactions with *Ruppia maritima* (widgeongrass). Estuar Coasts 37:20–30
Moreno-Marín F, Brun FG, Pedersen MF (2018) Additive response to multiple environmental stressors in the seagrass *Zostera marina* L. Limnol Oceanogr 63:1528–1544
Murray L, Wetzel RL (1987) Oxygen production and consumption associated with the major autotrophic components in two temperate seagrass communities. Mar Ecol Prog Ser 38:231–239
Nejrup LB, Pedersen MF (2008) Effects of salinity and water temperature on the ecological performance of *Zostera marina.* Aquat Bot 88:239–246
Nguyen HM, Kim M, Ralph PJ, Marín-Guirao L, Pernice M, Procaccini G (2020) Stress memory in seagrasses: first insight into the effects of thermal priming and the role of epigenetic modifications. Front Plant Sci 11:494
Niu S, Zhang P, Liu J, Guo D, Zhang X (2012) The effect of temperature on the survival, growth, photosynthesis, and respiration of young seedlings of eelgrass *Zostera marina* L. Aquaculture 350–353:98–108
Oliver ECJ, Burrows MT, Donat MG, Sen Gupta A and others (2019) Projected marine heatwaves in the 21st century and the potential for ecological impact. Front Mar Sci 6:734
Oreska MPJ, McGlathery KJ, Porter JH, Asmus H, Asmus RM, Vaquer A (2017) Seagrass blue carbon spatial patterns at the meadow-scale. PLOS ONE 12:e0176630
Oreska MPJ, McGlathery KJ, Wiberg PL, Orth RJ, Wilcox DJ (2021) Defining the *Zostera marina* (eelgrass) niche from long-term success of restored and naturally colonized meadows: implications for seagrass restoration. Estuar Coasts 44:396–411
Orth RJ, McGlathery KJ (2012) Eelgrass recovery in the coastal bays of the Virginia Coast Reserve, USA. Mar Ecol Prog Ser 448:173–176
Orth RJ, Lefcheck JS, McGlathery KS, Aoki LR and others (2020) Restoration of seagrass habitat leads to rapid recovery of coastal ecosystem services. Sci Adv 6:eabc6434
Pedersen O, Colmer TD, Borum J, Zavala-Perez A, Kendrick GA (2016) Heat stress of two tropical seagrass species during low tides—impact on underwater net photosynthesis, dark respiration and diel *in situ* internal aeration. New Phytol 210:1207–1218
Pendleton L, Donato DC, Murray BC, Crooks S and others (2012) Estimating global 'blue carbon' emissions from conversion and degradation of vegetated coastal ecosystems. PLOS ONE 7:e43542
Pregnall AM, Smith RD, Kursar TA, Alberte RS (1984) Metabolic adaptation of *Zostera marina* (eelgrass) to diurnal periods of root anoxia. Mar Biol 83:141–147
Qin LZ, Kim SH, Song HJ, Kim HG and others (2020) Long-term variability in the flowering phenology and intensity of the temperate seagrass *Zostera marina* in response to regional sea warming. Ecol Indic 119:106821

R Core Team (2017) R: a language and environment for statistical computing. R Foundation for Statistical Computing, Vienna

Rasmusson LM, Gullström M, Gunnarsson PCB, George R, Björk M (2019) Estimation of a whole plant Q10 to assess seagrass productivity during temperature shifts. Sci Rep 9:12667

Rasmusson LM, Buapet P, George R, Gullström M, Gunnarsson PCB, Björk M (2020) Effects of temperature and hypoxia on respiration, photorespiration, and photosynthesis of seagrass leaves from contrasting temperature regimes. ICES J Mar Sci 77:2056–2065

Rheuban JE, Berg P (2013) The effects of spatial and temporal variability at the sediment surface on aquatic eddy correlation flux measurements. Limnol Oceanogr Methods 11: 351–359

Rheuban JE, Berg P, McGlathery KJ (2014a) Ecosystem metabolism along a colonization gradient of eelgrass (*Zostera marina*) measured by eddy correlation. Limnol Oceanogr 59:1376–1387

Rheuban JE, Berg P, McGlathery KJ (2014b) Multiple timescale processes drive ecosystem metabolism in eelgrass (*Zostera marina*) meadows. Mar Ecol Prog Ser 507:1–13

Richardson JP, Lefcheck JS, Orth RJ (2018) Warming temperatures alter the relative abundance and distribution of two co-occurring foundational seagrasses in Chesapeake Bay, USA. Mar Ecol Prog Ser 599:65–74

Shields EC, Moore KA, Parrish DB (2018) Adaptations by *Zostera marina* dominated seagrass meadows in response to water quality and climate forcing. Diversity 10:125

Shields EC, Parrish D, Moore KA (2019) Short-term temperature stress results in seagrass community shift in a temperate estuary. Estuar Coasts 42:755–764

Sokolova IM (2013) Energy-limited tolerance to stress as a conceptual framework to integrate the effects of multiple stressors. Integr Comp Biol 53:597–608

Staehr PA, Borum J (2011) Seasonal acclimation in metabolism reduces light requirements of eelgrass (*Zostera marina*). J Exp Mar Biol Ecol 407:139–146

Volaric MP, Berg P, Reidenbach MA (2018) Oxygen metabolism of intertidal oyster reefs measured by aquatic eddy covariance. Mar Ecol Prog Ser 599:75–91

Wahid A, Gelani S, Ashraf M, Foolad MR (2007) Heat tolerance in plants: an overview. Environ Exp Bot 61: 199–223

Wilson KL, Lotze HK (2019) Climate change projections reveal range shifts of eelgrass *Zostera marina* in the Northwest Atlantic. Mar Ecol Prog Ser 620:47–62

York PH, Gruber RK, Hill R, Ralph PJ, Booth DJ, Macreadie PI (2013) Physiological and morphological responses of the temperate seagrass *Zostera muelleri* to multiple stressors: investigating the interactive effects of light and temperature. PLOS ONE 8:e76377

*Editorial responsibility: Just Cebrian, San Francisco, California, USA*
*Reviewed by: 2 anonymous referees*

*Submitted: December 3, 2023*
*Accepted: April 10, 2024*
*Proofs received from author(s): May 11, 2024*